Synthesis and Characterization of Titania Nanotubes with Au Nanoparticles

Fernando González-Zavala [a], Marcos Martínez-García [b], Luis Escobar Alarcón [c] and Tatiana E. Klimova [a*]

[a] *Laboratorio de Nanocatálisis, Departamento de Ingeniería Química, Facultad de Química, Universidad Nacional Autónoma de México (UNAM), Cd. Universitaria, Coyoacán, Ciudad de México-04510, México.*
[b] *Instituto de Química, Universidad Nacional Autónoma de México (UNAM), Cd. Universitaria, Coyoacán, Ciudad de México-04510, México.*
[c] *Instituto Nacional de Investigaciones Nucleares, Carretera México-Toluca km 36.5, Ocoyoacac, Mexico.*

Authors' contributions

This work was carried out in collaboration among all authors. Author FGZ designed the study, performed the synthesis of the supports and catalysts and their characterization, and wrote the first draft of the manuscript. Author MMG managed the literature searches and the analyses of the study, data validation and curation of the manuscript. Author LEA performed the photoluminescence (PL) studies of all the compounds. Author TEK managed supervision, project administration, funding acquisition, validation, writing - review and editing of the manuscript. All authors read and approved the final manuscript.

Original Research Article

ABSTRACT

TiO_2 nanotubes were prepared by hydrothermal synthesis and modified with different amounts of gold nanoparticles by deposition-precipitation with urea. The catalysts were characterized to determine the effect of the presence of Au nanoparticles on the physico-chemical characteristics of

---

the materials and their electron storage capability. Raman spectroscopy revealed the transformation of the trititanate structure into the titania anatase domains upon gold deposition. This transformation was enhanced by an increase in Au loading and the thermal treatment of the materials. The size of Au nanoparticles increased upon the reduction treatment. The presence of Au nanoparticles produced a slight narrowing of the energy bandgap of the titania nanotubular material and had an important effect on its photoluminescence properties, important for some practical applications. Photoluminescence spectroscopy showed that the presence of Au nanoparticles on the surface of titania nanotubes significantly delayed electron-hole recombination and increased the ability of materials for charge separation. Superior performance of Au-containing titania nanotubes was illustrated by the evaluation of their photocatalytic activity. Au-containing titania nanotubes showed enhanced photocatalytic activity in the degradation of methylene blue dye in aqueous solutions upon UV irradiation compared to the pristine nanotubes and the titania Degussa P25.

1. INTRODUCTION

"Titania-based materials have attracted much attention in the catalytic and biomedical fields, in experimental and theoretical research, due to their unique optical, chemical and physical properties. They also have high photocatalytic activity, due to the strong oxidizing properties and non-toxicity" [1-3]. "Anatase and rutile are the most studied polymorphs of titania for solar driven applications. Both of these polymorphs have indirect band gap, which is 3.0 eV for rutile and 3.2 eV for anatase, corresponding to the ultra-violet (UV) light region, limiting their use as daylight-activated photocatalysts" [4]. "Anatase is the most active phase for photocatalytic applications, due to its better electronic and chemical surface properties" [3]. To increase the activity of the titania materials, they have been modified with noble metals, non-metallic dopants, or forming nanostructured heterojunctions with other phases, all with good results [1,5-7].

In 1998 Kasuga et al. reported "the synthesis of TiO_2-based materials in nanotubular form employing hydrothermal synthesis in a highly alkaline environment" [8]. "Alkaline hydrothermal synthesis produces titanate nanotubes, which formally could be considered as hydrated forms of TiO_2. Since the exact crystal structure is currently disputed, this nanotubular material is referred to as both protonated titanate and TiO_2 nanomaterial. A clear advantage of the hydrothermal technique is the capability of near 100% conversion of the precursors to titanate nanotubes in one single process stage without involving the use of excessively high temperature or pressure" [9]. "These nanostructured materials present interesting properties, the negatively charged two-dimensional titanium-containing sheets separated by exchangeable cations in the interlayer spaces, which allows large ion-exchange capability, fast ion diffusion and high surface charge density. Another attractive feature of these titanate nanostructures is their ability of transformation back to titanium dioxide, allowing the use of titanates as flexible precursors for TiO_2 nano-engineering" [10-12].

"Titanate nanotubes combine the properties and applications of conventional TiO_2 nanoparticles (wide-bandgap semiconductor, chemical stability, solar harvesting, photocatalyst) with the properties of layered titanates (ion exchange)" [9]. However, it is reported that low-dimensional TiO_2 nanostructures tend to have a bandgap larger than 3.2 eV, because of the quantum confinement effect, resulting in low efficiency and limited use of UV light of the solar spectrum [13]. One strategy to improve their response to lower photon energy is the titania photosensitization with noble metal nanoparticles on their surface. Noble metal nanoparticles have unique electronic, optical and magnetic properties, as well as the strong absorption of visible light due to the surface plasmon resonance effect (SPR) improving the response in the visible range [14-17]. Their use presents advantages such as chemical stability, since noble metal nanoparticles are inert against photo-oxidation, which makes the catalysts more stable and durable. Mainly, Au, Pt, Pd and Rh are noble metals that do not present corrosion under photocatalytic conditions [18-22].

Different experimental techniques were used for the deposition of noble metal species on solid supports. Electrodeposition is a well-known

method to produce in situ metallic coatings by the action of an electric current on a conductive material immersed in a solution containing a salt of the metal to be deposited. The electrodeposited films have a high mechanical and chemical stability [23-25]. Other methods used for the preparation of materials modified with metal Au nanoparticles are supercritical CO_2 and wet impregnation [26], thermal atomic layer deposition [27], physical adsorption, cyclic voltammetry and chronoamperometry [28], electrophoresis deposition [29], vapor phase impregnation [30], etc.

The Au-decorated titania is a promising material, since it combines the physical (high surface area, band gap, surface plasmon resonance) and the chemical (stability, redox capability) properties of titanium dioxide and gold nanoparticles. R. Zanella et al. [31,32] prepared Au nanoparticles over nanostructured TiO_2 employing a deposition-precipitation with urea method with high metal loading (8 wt. %) and Au particle sizes of 2 nm. Then, the obtained catalysts were tested in CO oxidation at 5 °C temperature, finding that the catalyst shows the maximum conversion rate, when it was calcined at a temperature of 200°C and the gold species are in the oxidation state III.

M. Murdoch et al. [33] obtained Au nanoparticles with a size between 3–30 nm by a deposition–precipitation method (using urea as a basification agent) over TiO_2 anatase and rutile particles synthesized by the sol-gel process. They found that, in the photoreaction of hydrogen production from ethanol, Au nanoparticles of similar size on anatase showed a rate two orders of magnitude higher than that recorded for Au on rutile support. It was also observed that, when Au particle size is in the 3–12 nm range, it does not affect the photoreaction rate.

S. Oros-Ruiz et al. [34] deposited Au nanoparticles on commercial TiO_2 (Degussa P25) by deposition–precipitation with urea and studied the photocatalytic hydrogen production. The effect of parameters such as mass of catalyst, gold loading, thermal treatment, and atmosphere of treatment were evaluated. They found that with an optimal gold loading for the photocatalysts of 0.5 wt. % and the mass of catalyst in the reactor of 0.5 g/L in a water/methanol 1:1 vol. solution, the production of hydrogen was 1866 µ mol g^{-1} h^{-1}.

A. Sandoval et al. [35] prepared nanoparticles of gold decorating nano-structured anatase crystals

supported on titania nanotubes for use as a catalyst in the oxidation of CO. With an Au loading of 4 wt. % deposited by the deposition-precipitation method with urea, the obtained materials showed a high activity for the oxidation reaction of CO at low temperature (-10-100°C), which was ascribed to a good dispersion of Au and chemical stability at 25°C.

From the above described literature information it can be concluded that the deposition-precipitation with urea (DPU) is a methodology that permits the deposition of high metal loadings with a good dispersion and a small size of the nanoparticles, which results in a uniform distribution and low agglomeration of the nanoparticles allowing to decorate nanostructured titania photocatalysts with nonstructural modification [31,36].

In this work, titania nanotubes (TNT) were synthesized by the Kasuga method, and Au nanoparticles were supported on them by the deposition-precipitation with urea method. The Au/TNT catalysts were characterized by different physico-chemical methods in order to inquire into their characteristics and possible applications in catalysis and other fields. Finally, the catalysts were evaluated in photocatalytic degradation of methylene blue dye.

2. MATERIALS AND METHODS

2.1 Reagents

Titanium (IV) oxide anatase, tetrachloroauric acid trihydrate ($HAuCl_4 \cdot 3H_2O$), sodium hydroxide (NaOH), urea ($CO(NH_2)_2$), methylene blue dye ($C_{16}H_{18}ClN_3S\ 3H_2O$) were purchased from Sigma-Aldrich and used without further purification.

2.2 Synthesis of Support and Catalysts

The titania nanotubes (TNT) were synthesized by alkali treatment in hydrothermal conditions, as reported by Kasuga et al. [8]. Briefly, 10 g of commercial TiO_2 anatase nanopowder were mixed with 300 mL of a 10 M NaOH solution, followed by hydrothermal treatment in a Teflon-lined autoclave at 140 °C for 20 h upon constant stirring. After the hydrothermal reaction, the sodium titanate nanotubes were filtered in vacuum, washed several times with deionized water to eliminate the excess of non-reacted

caustic soda and dried at 120 °C for 6 h. To decrease Na content in the synthesized nanotubes, the dry precipitate was washed with 0.1 M HCl solution 2 times for 2 h, then filtered and washed with deionized water and dried at 120°C for 6 h.
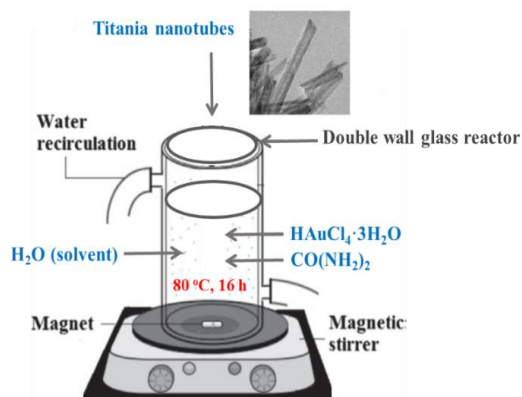

Fig. 1. Experimental setup for the deposition of Au nanoparticles on titania nanotubes by the DPU method

The deposition of the Au nanoparticles was performed by the deposition-precipitation with urea method (DPU) [32]. Fig. 1 shows the experimental setup used for the DPU preparation. In brief, 1 g of titania nanotubes (TNT) was dispersed in 50 mL of an aqueous solution of $HAuCl_4$ (4.2 x 10^{-3} M) and urea (0.42 M). This gold concentration corresponds to a 4 wt. % theoretical Au loading. The solution temperature was fixed at 80°C and the time of deposition-precipitation was 16 h under magnetic stirring. Afterwards, the solid material was separated from the precursor solution by centrifugation at 5000 rpm for 20 min, then washed with deionized water (100 mL per gram of the catalyst) at 50°C for 10 min and then centrifuged again for 30 min; this procedure was repeated 4 times. Finally, the catalysts were dried at 80°C for 2 h in a vacuum oven. Three catalysts with different theoretical Au loadings (0.5, 2 and 4 wt.%) were prepared and labeled as Au-x/TNT, where x is the theoretical Au loading. All the preparations were performed in the absence of light in order to avoid decomposition and reduction of gold precursors. For comparison purposes, a series of the as-prepared Au-x/TNT catalysts were activated (reduced) at 200 °C for 2 h in a H_2/Ar (70/30 v/v) atmosphere, in order to study the effect of the supported reduced metallic nanoparticles. Reduced samples are named as Au-x(R)/TNT.

2.3 Characterization of Support and Catalysts

N_2 adsorption-desorption isotherms were acquired with a Micromeritics 3-FLEX automatic analyzer at liquid N_2 temperature (-197.4°C). Prior to the sample analysis, the solids were degassed out in a N_2 stream (50 ml/min) at 250°C for 6 h. Specific surface areas were calculated by the BET method (S_{BET}). The total pore volume (V_P) was determined by nitrogen adsorption at a relative pressure of 0.98. Pore size distributions and average pore diameters (D_P) were determined from the desorption isotherms by the BJH method. The band gap of the materials was calculated from the F(R) diffuse reflectance spectra collected with a Varian Cary 100 UV-vis spectrophotometer equipped with an integration sphere attachment and polytetrafluoroethylene as a reference material. The microstructure of the materials was studied by Raman spectroscopy, the spectra were obtained using a micro-Raman Horiba Jobyn Ivon LabRam 800 system, equipped with a confocal microscope Olympus BX40 and a 100X objective. The samples were excited using the second harmonic of a Nd:YAG laser (532 nm). All spectra were calibrated using the 521 cm^{-1} lines of monocrystalline silicon. Spectral photoluminescence (PL) properties were studied by PL spectroscopy using a spectrofluorometer (FluoroMax 4, Horiba Jobyn Ivon) equipped with a 150 W Xenon lamp as excitation source. Emission spectra were acquired, by excitation at 310 nm, from 340 to 600 nm to avoid the first and second order of Rayleigh scattering. Powder XRD patterns were recorded in the 3°≤ 2θ≤ 80° range on a Siemens D500 diffractometer, using Cu*Kα* radiation (λ = 1.5406 Å) and a goniometer speed of 1° (2θ)/min. TEM images of the catalysts were recorded with a JEOL 2010 microscope (resolving power 1.9 Å at 200 kV). Chemical analysis of as synthesized nanotubes and Au-decorated catalysts was performed by SEM-EDS using a JEOL 5900 LV microscope with OXFORD ISIS equipment.

2.4 Photocatalytic Degradation of Methylene Blue Dye

The synthesized catalysts were evaluated in the photocatalytic degradation of methylene blue (MB) dye in aqueous solution. The photocatalytic reactions were carried out in a double wall cylindrical glass reactor connected to a recirculation bath maintaining 20°C temperature for the entire reaction time. In the reactor, 0.02 g

of catalyst was dispersed in 150 ml of an aqueous solution of MB dye (20 ppm concentration). As a UV light source, a pen ray Hg lamp with emission at 254 nm was used ($I_o=4400$ µW cm^{-2}). The lamp was submerged in a quartz tube holder in the center of the reactor. The adsorption-desorption equilibrium was reached in 2 h in the absence of light (the dark step). Aliquots of the solution were taken and analyzed every 40 min. After reaching the equilibrium, the solution was irradiated with UV light for 2 h. At this step, aliquots were taken at every 20 min. The course of the reaction was evaluated following the decrease of the intensity of the characteristic absorption band of the MB dye centered at 663 nm. Photocatalytic reactions were performed for the as-synthesized Au-x/TNT and reduced Au-x(R)/TNT catalysts. For comparison purposes, the commercial titania Degussa P25 was also evaluated.

3. RESULTS AND DISCUSSION

3.1 N$_2$ Adsorption-desorption Studies

The obtained isotherms from the N$_2$ adsorption-desorption showed that the as-synthesized titania nanotubes (TNT) had a type IV adsorption isotherm with a hysteresis loop combined by the H1 and H3 types, Fig. 2(a). This evidences the presence of materials with uniform nearly cylindrical mesopores (void spaces inside the nanotubes) and solids consisting of aggregates or agglomerates of particles forming slit-shaped pores of non-uniform size, respectively. No changes in the isotherms were observed after the deposition of Au by the DPU method. The pore size distributions of all materials (TNT and Au catalysts, regardless the Au content) presented a similar shape with bimodal pore distributions with two maxima (at about 34 and 49 Å) and a broad shoulder between 200 and 1000 Å (Fig. 2(b)). The first peak (34 Å) was attributed to the internal diameter of the prepared nanotubes, meanwhile the second one (49 Å) may correspond to the space between the titania nanotubes in their agglomerates, and finally large pores represent the spaces between the above agglomerates, Fig. 2(b).

The starting TNT material had 276 m^2/g surface area, 0.575 cm^3/g total pore volume and 83 Å average pore diameter, Table 1. After the deposition of Au, a slight decrease in the textural properties was observed. Thus, the catalyst with 4 wt. % Au loading showed 225 m^2/g surface area, 0.401 cm^3/g pore volume and 71 Å average pore diameter. This decrease could be attributed to the incorporation of Au nanoparticles on the TNT surface by the DPU method.
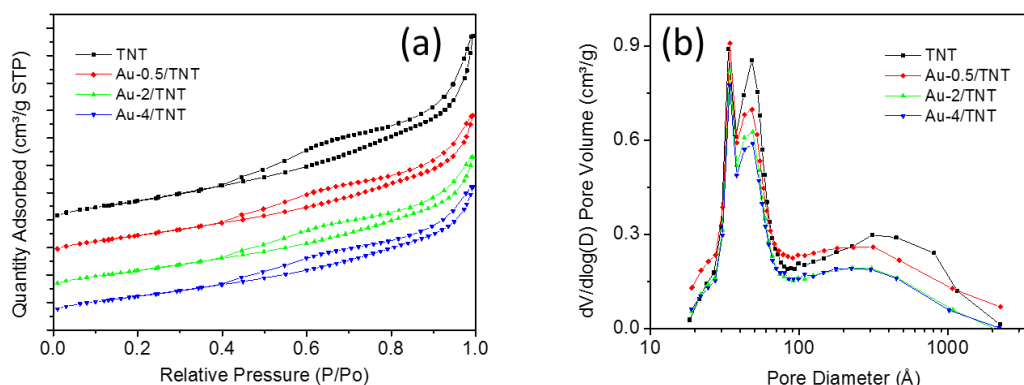

Fig. 2. N$_2$ adsorption-desorption isotherms (a) and pore size distributions (b) of TNT and Au-x/TNT catalysts

Table 1. Textural characteristics and chemical composition of TNT and Au-x/TNT materials

Sample	Textural characteristics			Au content (wt. %)		
	S$_{BET}$ (m^2/g)	D$_P$ (Å)	V$_P$ (cm^3/g)	Theoretical	Experimental	
					As-synthesized	Reduced
TNT	276	83	0.575	-	-	-
Au-0.5/TNT	244	72	0.436	0.5	0.56	0.53
Au-2/TNT	239	70	0.416	2.0	2.34	1.99
Au-4/TNT	225	71	0.401	4.0	4.07	4.11

3.2 Transmission Electron Microscopy Analysis

TEM micrographs of the Au-x/TNT (Fig. 3) show the presence of the agglomerates of multiwalled nanotubes with the averaged diameter of 100 nm and 1.5 μm length. After the DPU deposition of Au nanoparticles, no changes were observed in the support's morphology. In Figs. 3(a-c), corresponding to 0.5, 2 and 4 wt. % Au loadings, small grey spots of spherical gold nanoparticles can be observed on the nanotube's surface. The average size of the Au nanoparticles was found to increase with Au loading, varying from 1 nm for 0.5 wt. % Au loading to 3nm for the Au-4/TNT sample.

To observe the effect of the activation treatment at 200 °C for 2 h in H_2/Ar atmosphere on the characteristics of Au nanoparticles on the TNT, reduced catalysts were also studied by TEM. Figs. 3(d-f) show the obtained micrographs. A noticeable increase in the size of the Au nanoparticles can be clearly observed when comparing the images of the same catalyst before and after reduction. The smallest Au

particles (2.5 nm or more in diameter) were found for the Au-0.5/TNT-R sample, while the largest ones (up to 18 nm diameter) were detected in the Au-4/TNT-R after reduction. Therefore, it can be concluded that the reduction treatment performed in the present study has an important effect on the size of Au nanoparticles supported on TNT materials.

3.3 Scanning Electron Microscopy

Fig. 4 reveals the SEM images of the synthesized samples after Au deposition by the DPU method. In all the images, characteristic fiber-like morphology of titania nanotubes can be seen. Modification of the TNT material by the incorporation of different amounts of Au (0.5 – 4 wt. %) on the surface did not produce any visible alteration in nanotubular morphology of the support. The elemental chemical composition results are presented in Table 1. The results confirm that the real loadings of Au in the as-synthesized and reduced catalysts are very close to the theoretically expected values of 0.5, 2 and 4 wt. %.
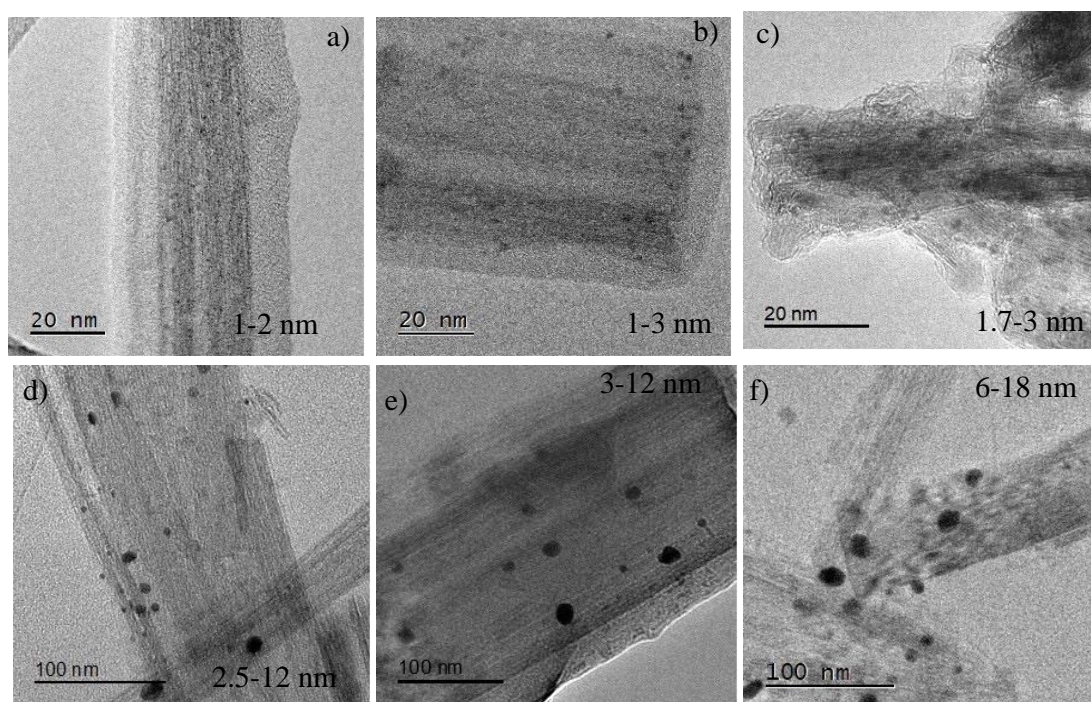

Fig. 3. TEM micrographs of the as-synthesized catalysts: (a) Au-0.5/TNT, (b) Au-2/TNT, (c) Au-4/TNT; and the same catalysts after reduction: (d) Au-0.5(R)/TNT, (e) Au-2(R)/TNT, (f) Au-4(R)/TNT. Observed intervals of Au particle sizes are shown for each catalyst on the corresponding image
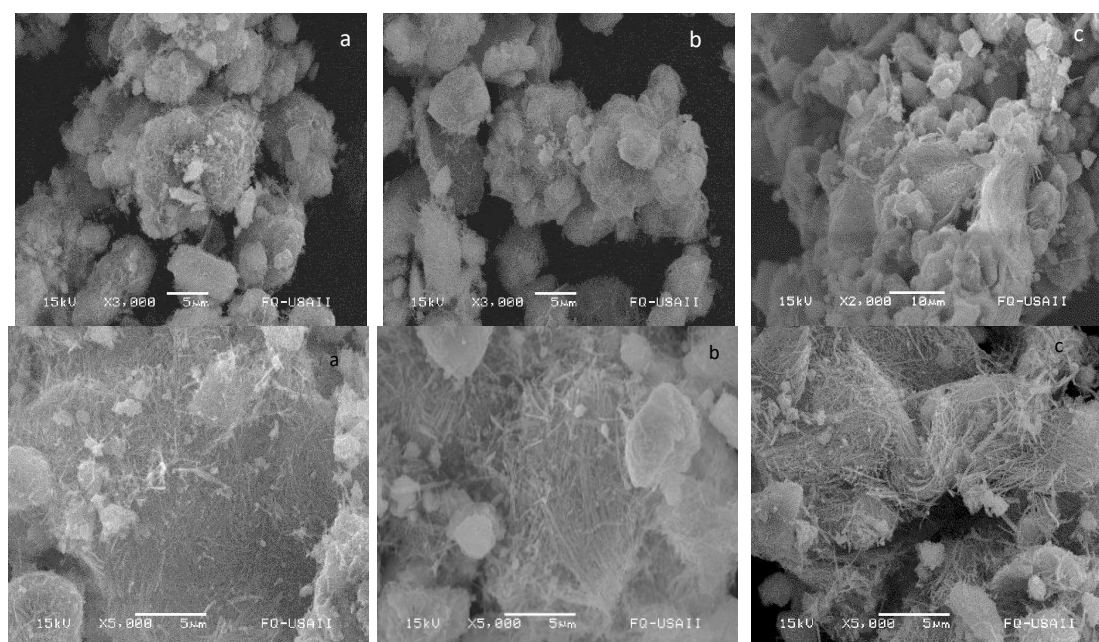
Fig. 4. SEM micrographs of as-synthesized Au-containing catalysts: (a) Au-0.5/TNT, (b) Au-2/TNT, (c) Au-4/TNT

3.4 Diffuse Reflectance Spectroscopy

Fig. 5(a) shows diffuse reflectance spectra of the TNT material and as-synthesized Au-x/TNT materials. The spectrum of the commercial titania Degussa P25 is also shown for comparison purposes. Only one broad signal can be observed in all the spectra in the 200-400 nm wavelength region. This signal corresponds to ligand-to-metal charge transfer (LMCT) from O^{2-} to Ti^{4+} of the titania-containing materials. From the obtained DR spectra shown in Fig. 5(a), the band gap energy (E_g) values were calculated using a modified Kubelka-Munk function for a direct allowed transition. The bang gap energy of the starting material, TNT, was 3.5 eV, slightly higher than the values of TiO_2 Degussa reference (3.3 eV). For the as-synthesized Au-x/TNT materials, a slight shift of the position of the absorption edge to higher wavelengths was observed comparted to the unmodified TNT support, and corresponding E_g values showed lower band gap energies (~3.4 eV). Regarding the signals attributable to the deposited Au nanoparticles, in the spectra of the as-synthesized Au-x/TNT materials they were not observed. The absence of a surface plasmon resonance (SPR) signals is in line with the very small size of Au nanoparticles in these samples, which was between 1 and 3 nm, according to the TEM observations, Figs. 3(a-c).
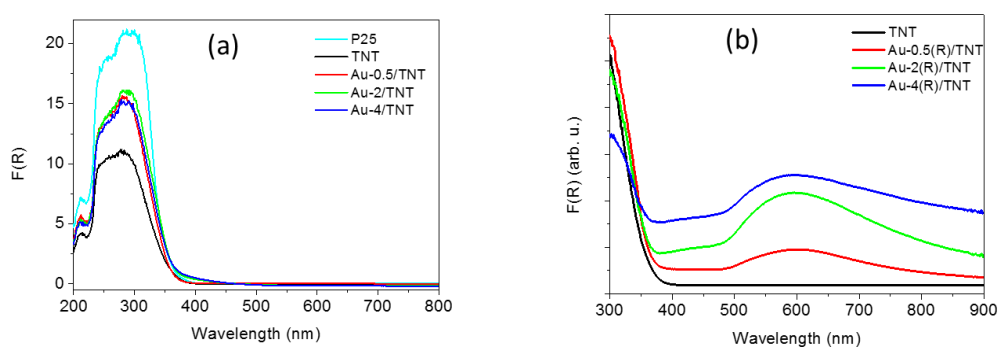

Fig. 5. Diffuse reflectance spectra of TNT and Au-x/TNT samples: (a) as-synthesized materials, (b) reduced materials. The spectrum of commercial titania Degussa P25 is also shown in chart (a) for comparison purposes

For the reduced Au-x(R)/TNT catalysts, Fig. 5(b), the LMCT signal of the TNT support did not suffer any changes. However, a broad signal centered at about 580 nm appeared, which is associated to the surface plasmon resonance SPR signal of the Au nanoparticles with a size between 5-20 nm [14]. This result points to an increase in the size of Au nanoparticles upon reduction treatment.

3.5 Powder X-ray Diffraction

Powder X-ray diffraction patterns of Au-x/TNT materials are shown in Fig. 6. For the as-synthesized materials, only typical diffraction lines of hydrous hydrogen trititanate crystalline structure ($H_2Ti_3O_7 \cdot xH_2O$, JCPDS No. 41-192) were observed, which are characteristic for the titania nanotubes prepared by the Kasuga method. The signals located at 10.0°, 24.4°, 48.3° (2θ) correspond to (200), (110) and (020) reflections of this crystalline phase. No signals corresponding to any Au crystalline phase were detected in the diffractograms of the as-synthesized materials.

For the reduced materials, Fig. 6(b), four new signals were observed in addition to the diffraction lines from the TNT material. Thus, the diffraction peaks at 38.3°, 46.7°, 65.3° and 79.9° (2θ) can be indexed to the (111), (200), (220), and (311) planes, respectively, of metallic Au crystalline phase (JCPDS No. 04-0784) [37]. The diffraction peak corresponding to the (111) crystal face, for all reduced catalysts was more

intense than it could be expected for the regular three-dimensional Au crystal. This observation about the relative intensity of the (111) and other diffraction signals indicates that the (111) plane was the predominant orientation of the reduced Au nanoparticles in the Au-x(R)/TNT samples.

3.6 FT-Raman Spectroscopy

The Raman spectra of the TNT material and as-synthesized Au-x/TNT are shown in Fig. 7(a). In the spectrum of the TNT sample, four main peaks centered at 190, 271, 450 and 664 cm^{-1} were observed. All these signals can be ascribed to vibrations of titanate nanotubular material, namely, the signal at 190 cm^{-1} is assigned to the lattice vibration mode [38,39] and the peaks at 271, 450 and 664 cm^{-1} correspond to the Ti-O-Ti stretching in the edge sharing corner of octahedral TiO_6 of $H_2Ti_3O_7$ [40]. After the deposition of Au species by the DPU method, a new signal at 147 cm^{-1} appeared. This signal was attributed previously to anatase in nanotubular form [30]. Its appearance indicates that after the DPU treatment, titania-like domains were formed in the TNT support. In addition, for the sample with the highest Au loading (4 wt. %), two bands centered at 400 and 600 cm^{-1} were detected, which could be attributed to the appearance of titanate nanowires [41]. These results point out to the microstructural changes in the TNT material upon deposition of different amounts of gold by the DPU method. These changes were not possible to detect by the XRD characterization described above, Fig. 6(a).
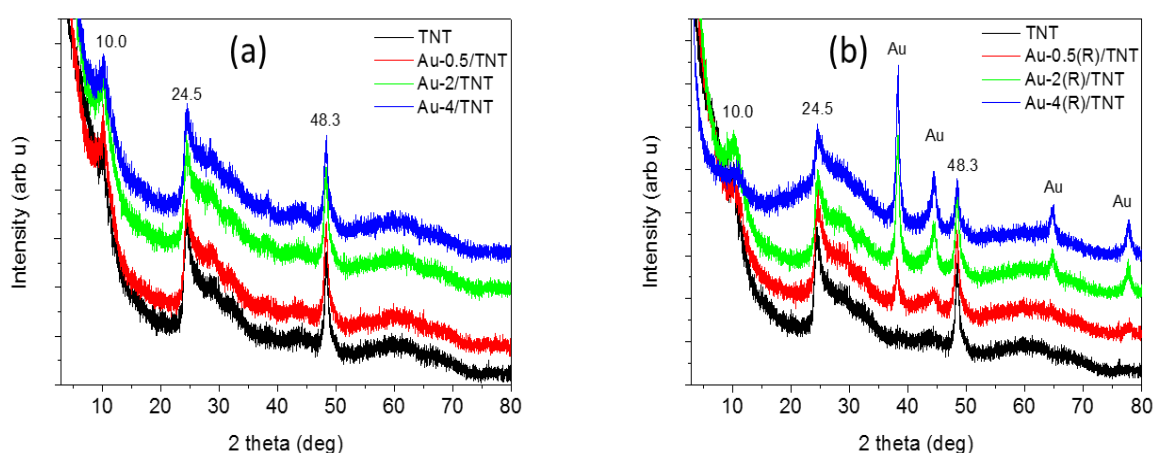

Fig. 6. X-ray diffraction patterns of (a) TNT and as-synthesized Au-x/TNT materials and (b) the same materials after reduction
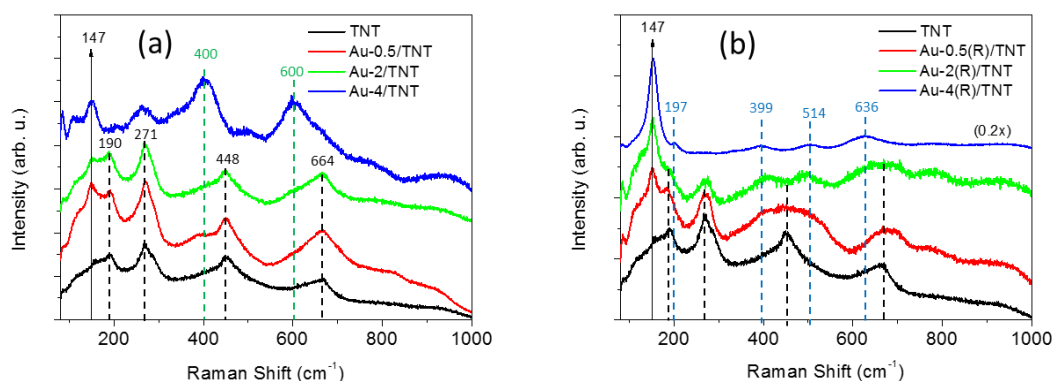
Fig. 7. FT-Raman spectra of (a) TNT and as-synthesized Au-x/TNT materials and (b) the same materials after reduction

In the case of the reduced Au-x(R)/TNT catalysts, Fig. 7(b), some new signals are observed in addition to those detected in the spectra of the as-synthesized samples, Fig. 7(a). Thus, in the spectra of the reduced Au-0.5(R)/TNT and Au-2(R)/TNT catalysts, signals at 399, 514 and 636 cm^{-1} appeared, in line with an increase in the intensity of the signal at 147 cm^{-1}. Therefore, a mixture of titanate nanotubes and some titania anatase domains are present in these samples. The reduction treatment at 200 ^{o}C for 2 h produced an increase in the amount and size of anatase microstructures in the samples. On the other hand, only the signals of TiO_2 anatase were detected in the spectrum of the reduced catalyst with 4 wt. % Au loading. Therefore, an increase in the gold loading in the samples promotes transformation of titanate nanotubes to anatase crystalline phase. This is in line with previous observations [41].

3.7 Photoluminescence Spectroscopy

Usually, when TiO_2 semiconductor is excited by ultraviolet light, electron/hole pairs are generated and then they suffer auto recombination. Photoluminescence (PL) is the emission of light during the recombination process, which can be used to study the fate of photogenerated electrons and holes in an excited semiconductor such as TiO_2 [42]. The photoluminescence intensity represents the recombination level of photogenerated carriers on the surface. Fig. 7(a) shows the photoluminescence spectra of the titania nanotubes (TNT) and the as-synthesized Au-x/TNT, in the wavelength range of 350-600 nm. In general, PL spectra show broad photoluminescence in the visible range (from 350 to 600 nm) with similar emission shapes, which indicates that similar types of defects are present in the studied materials. Decreased photoluminescence intensity was detected for all the Au-x/TNT materials modified with Au on the surface compared to the starting TNT support. This indicates that gold nanoparticles increase the ability of the TiO_2 for electron storage by preventing the direct recombination of electrons and holes [43]. The Au-4/TNT catalyst exhibits a slight increase in the photoluminescence intensity compared to Au-2/TNT and Au-0.5/TNT. This may be due to the larger amount of gold nanoparticles on the surface of the Au-4/TNT implying smaller spaces between the gold nanoparticles and their extra interactions, weakening the electron capture ability of gold nanoparticles in this sample [44]. The peaks observed in the PL spectra (Fig. 8) were assigned as follows: the first peak (396 nm) corresponds to band gap transition of titania nanotubes [45], the peak at 437 nm is due to the charge-transfer transition from Ti^{3+} to oxygen anion in the TiO_6 octahedra [46,47]. The signal at 560 nm may be attributed to the recombination of photo-generated holes with the electrons in singly occupied oxygen vacancies in the titania nanotubes [48,49].

In the case of the reduced Au-x(R)/TNT materials, Fig. 8(b), the photoluminescence intensity was drastically quenched by the reduction of Au species and an increase in the size of metal nanoparticles, as it was shown by TEM and XRD characterizations. The decrease in PL intensity can be explained by an improvement in electron hole separation resulting in delayed recombination of photogenerated charge carriers. Therefore, it may be expected that in some applications, for example, in photocatalysis, Au-decorated titania nanotubes would exhibit increased performance compared to that of the un-modified titania nanotubes [15,50].
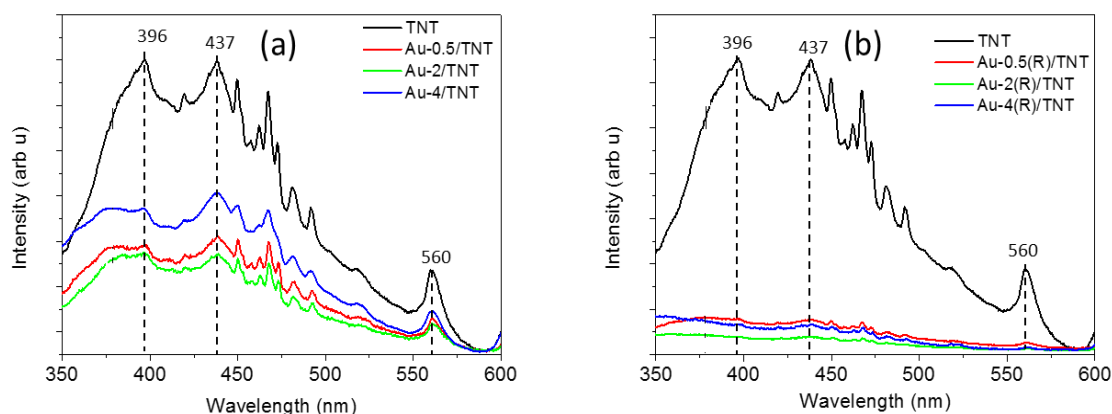
Fig. 8. Photoluminescence spectra of the TNT and Au-x/TNT catalysts with different Au contents (a) and the same catalysts after reduction (b)
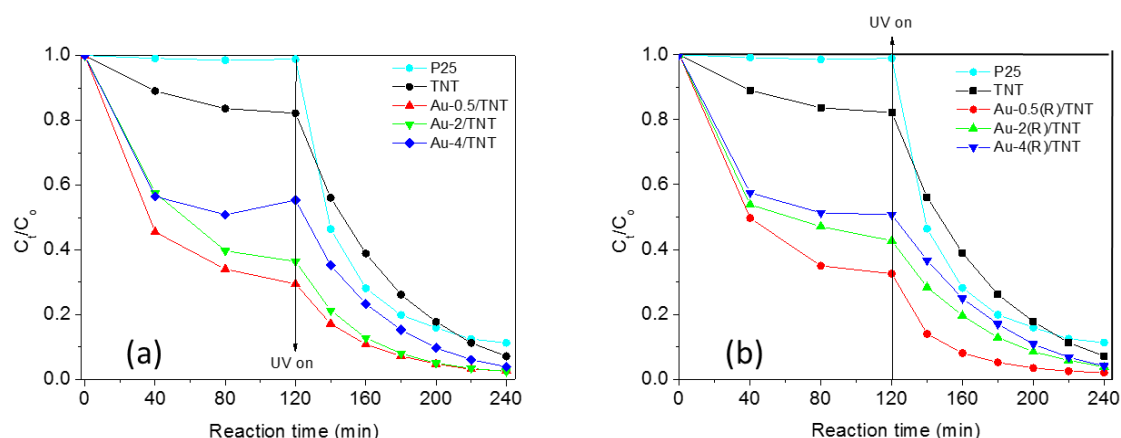

Fig. 9. Photocatalytic degradation of methylene blue dye in aqueous solution upon UV irradiation with the as-synthesized Au-x/TNT catalysts (a) and the same catalysts after reduction (b). The results obtained with the commercial titania Degussa P25 are also shown for comparison purposes

3.8 Photocatalytic Degradation of Methylene Blue Dye

Synthesized Au-containing catalysts and the starting TNT material were tested in the photocatalytic degradation of methylene blue (MB) dye in aqueous solution upon UV irradiation. For comparison purposes, titania Degussa P-25 was tested in the same conditions as the photocatalyst. Fig. 9 shows the obtained results. For all the catalysts, the experiments were performed in two steps. In the first one, the equilibrium of the MB adsorption on the catalyst was reached in the dark for 120 min. The objective of this step was to separate the adsorption of the dye from its photocatalytic degradation. For the titania Degussa P25, only a small amount (< 2%) of the initial MB was

adsorbed, while all materials containing Au deposited on titania nanotubes adsorbed much higher amounts of MB in the dark. The removal of MB at this stage was due to a cation exchange mechanism, which has been reported for the adsorption of cationic dyes on titanate nanotubes [51]. In addition, the presence of Au nanoparticles enhanced the adsorption of the MB dye, which was especially high on the catalysts with low Au loading (Au-0.5/TNT and Au-0.5(R)/TNT) and small nanoparticles' size. The reduction treatment of the Au-x/TNT catalysts slightly affected the amount of adsorbed MB, which decreased upon reduction, probably, due to an increase in the size of Au nanoparticles. Due to the different adsorption capacity of each Au-containing photocatalyst, the concentration of MB remaining in the solution after 120 min in the

dark was different for each one of the catalysts at the moment, when the UV irradiation was turned on (see Fig. 9). Upon UV irradiation, as expected, all Au-containing catalysts (as-synthesized and the reduced ones) resulted to be more active compared to the un-modified TNT semiconductor. This can be due to the delayed electron-hole recombination in the presence of Au nanoparticles. At the final reaction time (240 min), 97-98% of MB elimination was reached with all Au-containing samples. Finally, all the Au-containing catalysts resulted to be more efficient than the commercial titania Degussa P25 reference. In addition, the difference between the synthesized catalysts and the commercial analog is that the former ones reach MB elimination through both adsorption and photodegradation processes, while the P25 is not capable of MB adsorption and works mainly through the mechanism of MB degradation.

4. CONCLUSION

In this work, a facile and practical method for the preparation of titania nanotubes modified with Au nanoparticles is presented. Obtained real gold loadings in the Au-x/TNT materials was very close to the theoretically expected values. After the deposition of Au nanoparticles on the surface of TNT, no significant changes were observed neither in the textural properties of the materials (N_2 physisorption), nor in the present crystalline phases (XRD). However, a more detailed investigation by Raman spectroscopy reveals some microstructural changes in the materials modified with gold, namely, the transformation of trititanate structure into the titania anatase domains. This transformation was enhanced by an increase in Au loading in the samples and by the thermal treatment of the materials (200 $^{\circ}$C 2 h) in molecular H_2 atmosphere. The as-synthesized Au-x/TNT materials had Au nanoparticles in the range of 1 to 3 nm size, while, when the materials underwent the reduction treatment, gold agglomeration and an increase in the nanoparticle's size to 2.5-18 nm was observed (TEM). The presence of Au nanoparticles produced a slight narrowing of the energy bandgap of the TNT material (DRS), which changed from 3.5 eV (TNT) to ~3.4 eV (Au-x/TNT). However, the presence of Au nanoparticles on the TNT surface, their amount and size, had an important effect on the photoluminescence properties of the TNT material. According to PL spectroscopy characterization, the presence of Au nanoparticles in the as-synthesized Au-x/TNT

materials and, especially, in the Au-x(R)/TNT ones significantly delayed electron-hole recombination and increased the ability of materials for charge separation. This property of the Au-modified titania nanotubes may be of key importance for some of their practical applications. In the present work, this point was illustrated in an example of photocatalytic degradation of methylene blue dye in aqueous solutions upon UV irradiation, in which Au-containing catalysts showed enhanced catalytic activity compared to the un-modified TNT semiconductor and the commercial titania Degussa P25 reference.

ACKNOWLEDGEMENTS

COMPETING INTERESTS

Authors have declared that no competing interests exist.

REFERENCES

1. Zou X, Liu J, Su J, Zuo F, Chen J, Feng P. Facile Synthesis of Thermal- and Photostable Titania with Paramagnetic Oxygen Vacancies for Visible-Light Photocatalysis, Chem. Eur. J. 2013;19:2866-73.
    DOI:10.1002/chem.201202833
2. Razali M, Ismail NA, Amin KAM. Nanostructured TiO$_2$ Materials: Preparation, Properties and Potential Applications (3P's), Solid State Phenomena. 2017;266:84-9.
    Available: 10.4028/www.scientific.net/SSP.266.84
3. Kiwaan HA, Atwee TM, Azab EA, El-Bindary AA. Photocatalytic degradation of organic dyes in the presence of nanostructured titanium dioxide, Journal of Molecular Structure 2020;1200:127115.
    Available:10.1016/j.molstruc.2019.127115

4. Cargnello M, Montini T, Smolin SY, Priebe JB, Jaén JJD, Doan-Nguyen VVT, et al. Engineering titania nanostructure to tune and improve its photocatalytic activity, Proceedings of the National Academy of Sciences Apr 2016;113(15): 3966-71.

   Available:10.1073/pnas.1524806113

5. Elsalamony RA, Mahmoud SA. Preparation of nanostructured ruthenium doped titania for the photocatalytic degradation of 2-chlorophenol under visible light, Arabian Journal of Chemistry 2017;10:194–205.

   Available:dx.doi.org/10.1016/j.arabjc.2012.06.008

6. Sheikh MUD, Naikoo GA, Bano TM, Khan F, Solar Assisted Photocatalytic reduction of Methyl Orange Molly Azo Dye over Porous TiO_2 nanostructures, New Journal of Chemistry. 2016;40(6): 5483–94.

   DOI:10.1039/c5nj03513a

7. Bavykin DV, Friedrich JM, Walsh FC. Protonated Titanates and TiO_2 Nanostructured Materials: Synthesis, Properties, and Applications, Adv. Mater. 2006;18:2807–24.

   Available: 10.1002/adma.200502696

8. Kasuga T, Hiramatsu M, Hoson A, Sekino T, Niihara K. Formation of Titanium Oxide Nanotube, Langmuir. 1998;14: 3160–3.

   Available: doi.org/10.1021/la9713816

9. Zhang Y, Jiang Z, Huang J, Lim LY, Li W, Deng J, et al. Titanate and Titania Nanostructured Materials for Environmental and Energy Applications: A Review, RSC Adv. 2015;5:79479-510.

   Available: doi.org/10.1039/C5RA11298B

10. Li N, Zhang L, Chen Y, Fang M, Zhang J, Wang H. Highly Efficient, Irreversible and Selective Ion Exchange Property of Layered Titanate Nanostructures, Adv. Funct. Mater. 2012;22:835–41.

    Available:10.1002/adfm.201102272

11. Sasaki T, Watanabe M. Semiconductor Nanosheet Crystallites of Quasi-TiO_2 and Their Optical Properties, J. Phys. Chem. B 1997;101:10159-61.

    Available:10.1021/jp9727658

12. Zhu HY, Lan Y, Gao XP, Ringer SP, Zheng ZF, Song DY, et al. Phase Transition between Nanostructures of Titanate and Titanium Dioxides via Simple Wet-Chemical Reactions, J. Am. Chem. Soc. 2005;127:6730–6.

    Available:10.1002/adfm.201102272

13. Fang J, Cao S-W, Wang Z, Shahjamali MM, Loo SCJ, Barber J, et al. Mesoporous plasmonic Au–TiO_2 nanocomposites for efficient visible-light-driven photocatalytic water reduction, International Journal of Hydrogen Energy, 2012;37:17853-61.

    Available:10.1016/j.ijhydene.2012.09.023

14. Du L, Furube A, Yamamoto K, Hara K, Katoh R, Tachiya M. Plasmon-Induced Charge Separation and Recombination Dynamics in Gold-TiO_2 Nanoparticle Systems: Dependence on TiO_2 Particle Size, J. Phys. Chem. C 2009;113: 6454–62.

    Available:10.1021/jp810576s

15. Mubeen S, Hernandez-Sosa G, Moses D, Lee J, Moskovits M. Plasmonic Photosensitization of a Wide Band Gap Semiconductor: Converting Plasmons to Charge Carriers, Nano Lett. 2011;11: 5548–52.

    Available:10.1021/nl203457v

16. Silva CG, Juárez R, Marino T, Molinari R, García H. Influence of Excitation Wavelength (UV or Visible Light) on the Photocatalytic Activity of Titania Containing Gold Nanoparticles for the Generation of Hydrogen or Oxygen from Water. J. Amer. Chem. Soc. 2011;133: 595-602.

    Available:10.1021/ja1086358

17. Ghosh SK, Pal T. Interparticle Coupling Effect on the Surface Plasmon Resonance of Gold Nanoparticles: From Theory to Applications, Chem. Rev. 2007;107: 4797–862.

    Available:10.1021/jp810576s

18. Feng C, Li G, Ren P, Wang Y, Huang X, Li D. Effect of photo-corrosion of Ag_2CO_3 on visible light photocatalytic activity of two kinds of Ag_2CO_3/TiO_2 prepared from different precursors, Appl. Catal. B 2014;158–159:224–32.

    Available:10.1016/j.apcatb.2014.04.020

19. Zhao Q, Li M, Chu J, Jiang T, Yin H. Preparation, characterization of Au (or Pt)-loaded titania nanotubes and their photocatalytic activities for degradation of methyl orange, Applied Surface Science 2009;255:3773–8.

Available:10.1016/j.apsusc.2008.10.044

20. Fornari AMD, de Araujo MB, Duarte CB, Machado G, Teixeira SR, Weibel DE. Photocatalytic reforming of aqueous formaldehyde with hydrogen generation over TiO_2 nanotubes loaded with Pt or Au nanoparticles, Int. J. Hydrog. 2016;41: 11599-607.

    Available:dx.doi.org/10.1016/j.ijhydene.2016.02.055

21. Lee J-H, Youn J-Il, Kim Y-J, Oh H-J. Effect of Palladium Nanoparticles on Photocatalytic Characteristics of N doped Titania Catalyst, Journal of Materials Science and Technology 2015;31: 664-9.

    Available:doi.org/10.1016/j.jmst.2014.11.023

22. László B, Baán K, Oszkó A, Erdőhelyi A, Kiss J, Kónya Z. Hydrogen evolution in the photocatalytic reaction between methane and water in the presence of CO_2 on titanate and titania supported Rh and Au catalysts, Topics in Catalysis 2018;61: 875–88.

    Available:doi.org/10.1007/s11244-018-0936-z

23. Babakhanian A, Kaki S, Ahmadi M, Ehzari H, Pashabadi A. Development of α-polyoxometalate–polypyrrole–Au nanoparticles modified sensor applied for detection of folic acid, Biosensors and Bioelectronics 2014;60: 185-90.

    Available:https://doi.org/10.1016/j.bios.2014.03.058

24. Azizi Z, Babakhanian A. Fabricating a new electrochemically modified pencil graphite electrode based on acetophenone (2,4-dinitrophenyl) hydrazone for determining selenium in food and water samples, Anal. Methods 2018;10: 5205-13.

    Available:https://doi.org/10.1039/C8AY01959B

25. Rostami-Javanroudi S, Babakhanian A. New electrochemical sensor for direct quantification of vitamin K in human blood serum, Microchemical Journal 2021;163: 105716.

    Available:https://doi.org/10.1016/j.microc.2020.105716

26. Huerta A, Torralvo MJ, Tenorio MJ, Pérez E, Bermúdez J, Calvo L, Cabañas A. Deposition of Au nanoparticles into mesoporous SiO_2 SBA-15, J. Supercrit. Fluids 2022;184:105582.

    Available:https://doi.org/10.1016/j.supflu.2022.105582

27. Hashemi FSM, Grillo F, Ravikumar VR, Benz A, Shekhar A, Griffiths MBE, Barryc ST, Ruud van Ommen J. Thermal atomic layer deposition of gold nanoparticles: controlled growth and size selection for photocatalysis, Nanoscale 2020;12: 9005-13.

    DOI: 10.1039/d0nr01092h

28. Paradowska E, Arkusz K, Pijanowska DG. Comparison of Gold Nanoparticles Deposition Methods and Their Influence on Electrochemical and Adsorption Properties of Titanium Dioxide Nanotubes, Materials 2020;13(19):4269. 10.3390/ma13194269

29. Thang NCM, Linh LG, Anh NH, Nguyen HLT, Hai LV, Hoang NT. Electrophoresis deposition of Au-nanoparticles on FTO electrode for As(III) detection, Vietnam J. Chem. 2023;61(1):93-100.

    Available:https://doi.org/10.1002/vjch.202200043

30. Hernández-Cruz MG, Solís-Casados DA, Toledo-Antonio JA, Vargas-García JR, Estrada-Flores M, Ángeles-Chávez C, Cortés-Jácome MA, Encarnación-Gómez C. Malachite Green Dye Decoloration over Au/TiO_2-Nanotubes Photocatalyst under Simulate Visible-Light Irradiation, Materials 2022;15:6209.

    Available:https://doi.org/10.3390/ma15186209

31. Zanella R, Giorgio S, Henry CR, Louis C. Alternative Methods for the Preparation of Gold Nanoparticles Supported on TiO_2, J. Phys. Chem. B 2002;106:7634-42.

    Available:10.1021/jp0144810

32. Zanella R, Giorgio S, Shin C-H, Henry CR, Louis C. Characterization and reactivity in CO oxidation of gold nanoparticles supported on TiO_2 prepared by deposition-precipitation with NaOH and urea, Journal of Catalysis 2004;222:357–67.

    Available:10.1016/j.jcat.2003.11.005

33. Murdoch M, Waterhouse GIN, Nadeem MA, Metson JB, Keane MA, Howe RF, et al. The effect of gold loading and particle size on photocatalytic hydrogen production from ethanol over Au/TiO_2 nanoparticles, Nat. Chem. 2011;3:489-92.

    Available:10.1038/NCHEM.1048

34. Oros-Ruiz S, Zanella R, López R, Hernández-Gordillo A, Gómez R. Photocatalytic hydrogen production by water/methanol decomposition using Au/TiO$_2$ prepared by deposition–precipitation with urea, Journal of Hazardous Materials, 2013;263P:2–10.
Available:https://doi.org/10.1016/j.jhazmat.2013.03.057

35. Sandoval A, Zanella R, Klimova TE. Titania nanotubes decorated with anatase nanocrystals as support for active and stable gold catalysts for CO oxidation, Catalysis Today 2017;282:140–50.
Available:http://dx.doi.org/10.1016/j.cattod.2016.05.056

36. Zanella R, Delannoy L, Louis C. Mechanism of deposition of gold precursors onto TiO$_2$ during the preparation by cation adsorption and deposition–precipitation with NaOH and urea, Applied Catalysis A: General 2005;291:62–72.
Available:10.1016/j.apcata.2005.02.045

37. Ren X, Song Y, Liu A, Zhang J, Yang P, Zhang J, et al. Experimental and theoretical studies of DMH as a complexing agent for a cyanide-free gold electroplating electrolyte, RSC Adv. 2015;5:64997–5004.
DOI: 10.1039/c5ra13140e

38. Qian L, Du Z-L, Yang S-Y, Jin Z-S. Raman study of titania nanotube by soft chemical process, Journal of Molecular Structure 2005;749:103–7.
Available:10.1016/j.molstruc.2005.04.002

39. Viana BC, Ferreira OP, Filho AGS, Hidalgo AA, Mendes FS, Alves OL. Alkali metal intercalated titanate nanotubes: A vibrational spectroscopy study, Vibrational Spectroscopy. 2011:55: 183–7.
Available:10.1016/j.vibspec.2010.11.007

40. Gao T, Fjellvåg H, Norby P. Crystal Structures of Titanate Nanotubes: A Raman Scattering Study, Inorg. Chem. 2009;48:1423-32.
Available: 10.1021/ic801508k

41. Pusztai P, Puskás R, Varga E, Erdöhelyi A, Kukovecz Á, Kónya Z, et al. Influence of gold additives on the stability and phase transformation of titanate nanostructures, Phys. Chem. Chem. Phys. 2014;16:26786.

42. Li FB, Li XZ. Photocatalytic properties of gold/gold ion-modified titanium dioxide for wastewater treatment, Appl. Catal. A Gen. 2002;228:15-27.
Available:https://doi.org/10.1016/S0926-860X(01)00953-X

43. Cao H, Qiao Y, Liu X, Lu T, Cui T, Meng F, et al. Electron storage mediated dark antibacterial action of bound silver nanoparticles: smaller is not always better, Acta Biomater. 2013;9:5100–10.
Available:https://doi.org/10.1016/j.actbio.2012.10.017

44. Cao H, Qiao Y, Meng F, Liu X. Spacing-dependent antimicrobial efficacy of immobilized silver nanoparticles, J. Phys. Chem. Lett. 2014;5:743–8.
Available:https://doi.org/10.1021/jz5000269

45. Hajjaji A, Elabidi M, Trabelsi K, Assadi AA, Bessais B, Rtimi S. Bacterial adhesion and inactivation on Ag decorated TiO$_2$-nanotubes under visible light: Effect of the nanotubes geometry on the photocatalytic activity, Colloids and Surfaces B: Biointerfaces 2018;170: 92–8.
Available:https://doi.org/10.1016/j.colsurfb.2018.06.005

46. Cheng L, Zhang D, Liao Y, Li F, Zhang H, Xiang Q. Constructing functionalized plasmonic gold/titanium dioxide nanosheets with small gold nanoparticles for efficient photocatalytic hydrogen evolution, Journal of Colloid and Interface Science 2019;555:94-103.
Available:https://doi.org/10.1016/j.jcis.2019.07.060

47. Pugazhenthiran N, Murugesan S, Anandan S. High surface area Ag-TiO$_2$ nanotubes for solar/visible-light photocatalytic degradation of ceftiofur sodium, Journal of Hazardous Materials 2013;263:541-9.
Available:http://dx.doi.org/10.1016/j.jhazmat.2013.10.011

48. Bavykin DV, Gordeev SN, Moskalenko AV, Lapkin AA, Walsh FC. Apparent Two-Dimensional Behavior of TiO$_2$ Nanotubes Revealed by Light Absorption and Luminescence, J. Phys. Chem. B. 2005;109:8565-9.
Available:10.1021/jp050762m

49. Yu Y, Wen W, Qian XY, Liu JB, Wu JM. UV and visible light photocatalytic activity

Available:10.1039/c4cp04084h

of Au/TiO$_2$ nanoforests with Anatase/Rutile phase junctions and controlled Au locations, Scientific Reports. 2017;7: 41253.

Available:10.1038/srep41253

50. Sang NX, Huong PTL, Thy TTM, Dat PT, Minh VC, Tho NH. Crystalline deformation and photoluminescence of titanium dioxide nanotubes during in situ hybridization with graphene: An example of the heterogeneous photocatalyst,

Superlattices and Microstructures. 2018; 121:9-15.

Available:https://doi.org/10.1016/j.spmi.201 8.07.020

51. Sandoval A, Hernández-Ventura C, Klimova TE. Titanate nanotubes for removal of methylene blue dye by combined adsorption and photocatalysis, Fuel. 2017;198:22-30.

Available:http://dx.doi.org/10.1016/j.fuel.20 16.11.007

Peer-review history:
The peer review history for this paper can be accessed here:
https://www.sdiarticle5.com/review-history/103391